

The Organization of Actin Filaments in the Stereocilia of Cochlear Hair Cells

LEWIS G. TILNEY, DAVID J. DEROSIER, and MICHAEL J. MULROY

Department of Biology, University of Pennsylvania, Philadelphia, Pennsylvania 19104; The Rosenstiel Center, Brandeis University, Waltham, Massachusetts 02154; Department of Anatomy, Medical Center, University of Massachusetts, Worcester, Massachusetts 01605

ABSTRACT Within each tapering stereocilium of the cochlea of the alligator lizard is a bundle of actin filaments with >3,000 filaments near the tip and only 18–29 filaments at the base where the bundle enters into the cuticular plate; there the filaments splay out as if on the surface of a cone, forming the rootlet. Decoration of the hair cells with subfragment 1 of myosin reveals that all the filaments in the stereocilia, including those that extend into the cuticular plate forming the rootlet, have unidirectional polarity, with the arrowheads pointing towards the cell center. The rest of the cuticular plate is composed of actin filaments that show random polarity, and numerous fine, 30 Å filaments that connect the rootlet filaments to each other, to the cuticular plate, and to the membrane. A careful examination of the packing of the actin filaments in the stereocilia by thin section and by optical diffraction reveals that the filaments are packed in a paracrystalline array with the crossover points of all the actin helices in near-perfect register. In transverse sections, the actin filaments are not hexagonally packed but, rather, are arranged in scalloped rows that present a festooned profile. We demonstrated that this profile is a product of the crossbridges by examining serial sections, sections of different thicknesses, and the same stereocilium at two different cutting angles. The filament packing is not altered by fixation in different media, removal of the limiting membrane by detergent extraction, or incubation of extracted hair cells in EGTA, EDTA, and Ca^{++} and ATP. From our results, we conclude that the stereocilia of the ear, unlike the brush border of intestinal epithelial cells, are not designed to shorten, nor do the filaments appear to slide past one another. In fact, the stereocilium is like a large, rigid structure designed to move as a lever.

There are 3–10 rows of stereocilia on the apical surface of each hair cell in the cochlea (organ of Corti) and a single cilium, the “kinocilium.” The latter is present in submammalian vertebrates and in developing mammals but not in the mature mammalian cochlea. Within each stereocilium is a population of filaments (7). The stereocilium, then, resembles a large microvillus rather than a cilium, but because the word stereocilium is firmly entrenched in the literature, we will continue to use it, although it is misleading. The filaments in the stereocilia of the equilibrium organ have recently been identified as actin filaments by their ability to decorate with myosin subfragment 1 (S1) (9). Where it could be determined, the arrowheads produced from the interaction of S1 with the actin filaments appeared to point towards the cell center indicating the polarity of the actin filaments. From these observations, Flock and Cheung (9) proposed that there is a similarity

between the stereocilia of the equilibrium organ and microvilli present in the apical surface of intestinal epithelial cells (20). This latter preparation is capable of movement *in vitro* (18). The hair cells in the equilibrium organ, in the lateral-line system of fishes and aquatic amphibians (see reference 8), and in the cochlea (see reference 8) all have a similar morphology. Accordingly, Flock and Cheung (9) suggested a functional homology among the stereocilia in the lateral line, in the equilibrium organ, in the cochlea, and in microvilli on intestinal epithelial cells, a contention with which we disagree.

Our initial reason for investigating the stereocilia was that they represent another example of a highly ordered bundle of actin filaments. As we began a characterization of this unique bundle of actin filaments, it became clear that an understanding of the structure of the stereocilium is essential for a determination of the mechanism of mechanical input into the cell. In

particular, we wondered whether the structure of the actin filament bundle plays a role in fine frequency discrimination (the so-called second filter). We, therefore, began an exploration of the hair cells in the cochlea to see whether the arrangement of the actin filaments in the stereocilia might effect their stiffness and motion. We chose the alligator lizard as our experimental system for three reasons. First, the stereocilia in the ear of this organism are among the longest on record, 31 μm in length (21). Second, experimental manipulations can be easily carried out, because the cochlea is readily accessible (22). Third, lizard ears are unusual in that frequency selectivity (the primary filter) is not related to the basilar membrane.

Our first step was to analyze the morphology of the stereocilia and the apical surface of the hair cells in the cochlea or, more specifically, in the basilar papilla using thin sections of intact, detergent-extracted, and S1-decorated papillae. We then carefully analyzed the packing of the actin filaments within the stereocilia by use of optical-diffraction and thin-sectioning techniques and tried to see whether we could alter the packing by incubating the demembrated ear in solutions that might physiologically change the packing or whether in vitro movements of the filament bundles could be induced as in intestinal microvilli (18).

These observations show that there are similarities between the stereocilia in the ear and the microvilli in intestinal epithelial cells but, more importantly, there are striking differences, many of which clearly relate to the functional properties of these two cell types. More specifically, motile events such as the shortening seen to occur in microvilli of intestinal epithelial cells are not applicable to the ear. Rather, the stereocilium is a large, rigid structure designed to move like a lever. More unexpected is that the packing of the actin filaments in the stereocilia is strikingly different from that in any of the other biological systems previously studied.

MATERIALS AND METHODS

Organisms

Alligator lizards (*Gerrhonotus multicarinatus*) purchased from Western Zoological Supply Co. (Monrovia, Calif.) were anesthetized with sodium pentobarbital (Nembutal) at a dosage of 0.07 mg/g of body weight. The cochlear duct was removed, using the dissection technique described by Miller (16), and the adjacent tissue was dissected away from the basilar papilla with fine forceps and scissors. The basilar papilla was then fixed, detergent extracted, or handled according to the procedures described below. In one case the stapes was removed, the round window membrane was cut through, and fixative was perfused through the cochlea before the cochlear duct was removed.

Preparation of S1

S1 was isolated and purified after the method of Murray (23), which was modified from Lowey et al. (15). The S1 was generously supplied by Dr. Annemarie Weber of the University of Pennsylvania.

Decoration with S1

The papilla was first incubated in Triton X-100 (Sigma Chemical Co., St. Louis, Mo.) in 30 mM Tris-HCl and 3 mM MgCl_2 at pH 7.5 for 5–10 min, then washed in buffer containing 3 mM Mg^{++} , and incubated in 4 mg/ml S1 in 0.05 M phosphate buffer at pH 6.8 for 1 h at 0°C. The papilla was then rinsed in phosphate buffer twice to remove unbound S1, fixed in 1% glutaraldehyde in 0.1 M phosphate buffer containing 2% tannic acid at pH 6.8 for 45 min (2), washed in cold buffer, postfixed in 1% OsO_4 in 0.1 M phosphate buffer at pH 6.4 for 45 min at 0°C, washed three times in distilled water, and stained en bloc with 0.5% uranyl acetate for 2–3 h at 0°C. The tissue was then dehydrated in acetone and embedded.

Fixation

A number of different fixation conditions before and after detergent extraction as well as after detergent extraction and incubation in various media were attempted. The reasons for using these procedures will be discussed in different sections of Results. In each case, at least two papillae were fixed so that transverse and longitudinal sections could be observed.

THE INTACT PAPILLA: (a) A 2% paraformaldehyde, 2% glutaraldehyde in 0.1 M phosphate buffer at pH 7.4 was perfused through the oval window; the papilla was then dissected out and immersed in the fixative. Fixation was carried out at room temperature initially, then at 4°C overnight. The tissue was then washed in 0.1 M phosphate buffer at pH 6.4 and fixed in 1% OsO_4 in phosphate buffer for 1 h 15 min at 0°C. The tissue was washed in distilled water and stained en bloc in 0.5% uranyl acetate overnight, dehydrated, and embedded the next day.

(b) The papillae were fixed by immersion in 1% glutaraldehyde (8% stock from Electron Microscope Sciences, Fort Washington, Pa.) in 0.05 M phosphate buffer at pH 6.8 for 30 min, washed in 0.1 M phosphate buffer, postfixed in 1% OsO_4 in 0.1 M phosphate buffer at pH 6.3 for 45 min at 0°C, washed in distilled water, and stained en bloc in 0.5% uranyl acetate for 3 h. The tissue was rapidly dehydrated and embedded in Araldite.

(c) The papillae were fixed by immersion in a solution containing 1% OsO_4 , 1% glutaraldehyde in 0.1 M phosphate buffer at pH 6.3 for 40 min at 0°C. The tissue was then washed in distilled water, stained en bloc for 3 h at 0°C, rapidly dehydrated, and embedded. The fixative was made up immediately before use.

DETERGENT EXTRACTION: (d) The papillae were extracted with 1% Triton X-100, in 30 mM Tris and 5 mM MgCl_2 at pH 7.3 at 0°C for 10 min, fixed in 1% glutaraldehyde in 30 mM Tris and 1 mM MgCl_2 at pH 7.3 for 30 min, washed in 0.1 M phosphate buffer at pH 6.8, and postfixed in 1% OsO_4 in 0.1 M phosphate buffer at pH 6.3 for 40 min at 0°C. The preparation was then washed in distilled water, stained en bloc, dehydrated, and embedded as mentioned above.

(e) The papillae were extracted with 1% Triton X-100 in 30 mM Tris and 3 mM MgCl_2 at pH 7.5 at 0°C and incubated for 3 h in 30 mM Tris buffer containing 40 mM MgCl_2 . Fixation was carried out by the addition of glutaraldehyde to the above solution. The final concentration of the glutaraldehyde was 1%. The preparation was then washed in Tris- MgCl_2 buffer, postfixed in 1% OsO_4 in 0.1 M phosphate buffer at pH 6.3 for 45 min at 0°C, washed in distilled water, stained en bloc, dehydrated and embedded.

INCUBATION IN THE ABSENCE OF DIVALENT IONS: (f) The papillae were extracted with 1% Triton X-100 in 30 mM Tris containing 5 mM EDTA and 5 mM EGTA at pH 7.3 for 30 min at 0°C. At the end of the 30-min period, the papillae were fixed in 1% glutaraldehyde in 0.05 M phosphate buffer at pH 6.8, washed, and postfixed in 1% OsO_4 in 0.1 M phosphate buffer at pH 6.3 for 40 min at 0°C, washed in distilled water, stained en bloc, dehydrated, and embedded.

ADDITION OF Ca^{++} AND ATP TO THE DEMEMBRATED PAPILLAE: (g) Papillae were immersed in 1% Triton X-100 in 30 mM Tris, 3 mM CaCl_2 , 2 mM MgCl_2 , 1 mM ATP at pH 7.3 for 10 min, then fixed for 5 min in the above solution without Triton X-100 but with 1% glutaraldehyde. The papillae were then fixed for 30 min in 1% glutaraldehyde in 0.05 M phosphate buffer at pH 6.8 for 25 min, washed in buffer, postfixed in 1% OsO_4 in 0.1 M phosphate buffer at pH 6.3 for 40 min at 0°C, washed in distilled water, stained en bloc, dehydrated, and embedded.

(h) Papillae were immersed in 1% Triton X-100 in 30 mM Tris, 1 mM MgCl_2 at pH 7.3 for 15 min at 0°C with three changes, incubated for 10 min at room temperature in 30 mM Tris, 3 mM CaCl_2 , 2 mM MgCl_2 , 1 mM ATP at pH 7.2 for 10 min at 22°C, fixed in the above solution with 1% glutaraldehyde for 5 min, then fixed for 25 min in 1% glutaraldehyde in 0.05 M phosphate buffer at pH 6.8, washed, and postfixed in 1% OsO_4 in 0.1 M phosphate buffer at pH 6.3 for 40 min at 0°C. The papillae were then washed in distilled water, stained en bloc, dehydrated, and embedded.

Transmission Electron Microscopy

After dehydration, the papillae were flat-embedded in Araldite or Epon. The papillae could then be oriented on a Sorvall Porter-Blum II ultramicrotome (DuPont Co., Sorvall Biomedical Div., Wilmington, Del.). Thick sections were cut and then stained with toluidine blue. When the appropriate depth in the bloc was found, thin sections were cut with a diamond knife and the grey sections were collected on uncoated grids and stained with uranyl acetate and lead citrate. For each of the eight procedures at least two ears were examined, one sectioned longitudinally, the other transversely. The grids were examined primarily with a Philips 200 electron microscope. Some tilting of the sections was carried out by means of a Philips 301 electron microscope. Serial sections were collected on colloidal-coated slotted grids. Section thickness was measured after the method of Reedy (25). The microscope was calibrated by use of a standard grid containing 28,000 lines/in (Ernest F. Fullam, Inc., Schenectady, N. Y.) at the beginning of

this study and toward the end. Unfortunately, we found that the microscope had changed magnification by ~15% during this period.

Scanning Electron Microscopy

The papillae were prepared as described above in fixation procedure *a*, except that the tissue was rinsed in 2% tannic acid after the aldehyde fixation. After dehydration through a graded series to absolute ethanol, the papillae were critical-point dried in liquid carbon dioxide in a Samdri PVT-3 apparatus (Biodynamics Research Corp. Rockville, Md.), sputter coated with gold using a Hummer II instrument (Technics, Inc., Alexandria, Va.) that had been modified to a triode, and examined with an Etec Autoscan scanning electron microscope.

Diffraction

Diffraction patterns of the electron micrographs were made with a diffractometer, using a laser as a light source and a 35-mm camera to record the diffraction pattern. The system was designed and built by E. Salmon and D. DeRosier.

RESULTS

The Anatomy of the Lizard Ear

We are including in this subheading a brief summary of the basic anatomy of the hair cell in the lizard ear to aid the reader not familiar with this subject. Details can be found in Mulroy (21) and Bagger-Sjöback and Wersall (1). The new information included in this report begins in the next subheading.

The basilar papilla, the oblong organ containing the hair cells, measures ~4,000 μm in length and 50 μm in width. The papilla can be subdivided into two regions, apical and basal. The apical region is overlain by a tectorial membrane and responds to frequencies below 900 cycles/s (31); the maximum height of the stereocilia here is 7 μm . The basal region is not overlain by a tectorial membrane and the maximum height of the stereocilia on adjacent hair cells increases systematically from 12 μm at the basal end to 31 μm at the junction between the apical and basal regions. These cells respond to frequencies of 1,000–4,000 cycles/s (31).

Each hair cell (~150/ear) is isolated from the neighboring cells by a ring of supporting cells. The latter are connected to the hair cells and to adjacent supporting cells by gap junctions, tight junctions, and desmosomes (24). Microvilli, ~0.5 μm in length, extend from the apical surface of the supporting cells into the endolymphatic fluid (see Fig. 1 and 2).

The hair cells are much larger in diameter than the supporting cells (Fig. 1) and have, just beneath their apical surfaces, an extensive filamentous plate, the cuticular plate (Fig. 2). Whereas the apical surface of the cuticular plate is flat, the basal surface bulges out well into the cytoplasm (Fig. 2). Projecting from the central part of the plate are as many as 75 stereocilia (Fig. 1). These are organized into rows (the maximum number of rows encountered was 10). Each hair cell also has a single kinocilium (Fig. 1), which is anchored by a basal body located within the cytoplasm in a notch in the cuticular plate. The kinocilium lies within the row of longest stereocilia and its location marks the morphological polarity of the cell; that is, displacement of the stereocilia towards the kinocilium depolarizes the hair cell, displacement away from the kinocilium hyperpolarizes the cell (12).

The length of each stereocilium is precisely determined not only relative to the position of the hair cell on the basilar papilla, but also in relation to the particular row in which the stereocilium is found on a particular hair cell (Fig. 1). As is easily appreciated in Fig. 1, the stereocilia of adjacent rows are of different heights presenting a staircaselike profile. Further

complicating the situation is the fact that each stereocilium tapers. The tapering of the stereocilia is most pronounced near the cuticular plate. Each stereocilium, then, is shaped like a pencil with the sharpened point resting on the apical surface of the cell (Figs. 1 and 2). At the point of contact between the stereocilium and the cuticular plate, the filaments present in the stereocilia are embedded in a dense material and extend into the cuticular plate as a rootlet (Figs. 2 and 4).

New Observations Regarding the Stereocilia

With paraformaldehyde-glutaraldehyde fixation (procedure *a*) or conventional glutaraldehyde followed by OsO_4 fixation, information on the substructure of the stereocilia, the cuticular plate, and the rootlet is not easily obtained. However, if the more soluble materials are extracted and at the same time the filaments are better preserved as with our glutaraldehyde fixation technique (procedure *b*) or simultaneous glutaraldehyde- OsO_4 fixation (procedure *c*), or if the tissue is extracted first with detergent (procedure *d*) that will remove the membranes and unbound proteins and then fixed with our glutaraldehyde technique, new information can be readily obtained. With these techniques the stereocilia, which can measure up to 0.8 μm in diameter at the distal end and yet only 0.13 μm at its junction with the cuticular plate, are seen to contain a bundle of parallel filaments each of which measures $\sim 50 \pm 5 \text{ \AA}$ in diameter (Fig. 3). We have estimated from transverse sections that there can be >3,000 filaments within a single stereocilium (the actual count was 3,163). These filaments terminate at or near the membrane at the tip of the stereocilium (Fig. 3); sometimes (although most frequently this is not the case) the filaments terminate in some material of greater density. Because the stereocilia taper as they approach the cuticular plate, it seems reasonable to suggest that the filaments within the center of the stereocilium run from the distal end into the cuticular plate just as the lead of a pencil runs down the middle of the pencil, but the filaments at the periphery of the bundle terminate in a regular fashion. We, in fact, have confirmed this suggestion by an examination of S1-decorated stereocilia (see below). We can find no obvious morphological specializations at the point of contact between the terminating filaments in the taper and the plasma membrane.

The rootlet can be seen to consist of a parallel array of filaments embedded, at least near the point of contact, between the stereocilium and the cuticular plate in some denser material (Figs. 4 and 5). The filaments in the rootlet are arranged as if on the surface of a cone so that, in transverse sections, the filament bundle appears as a doughnut. In favorable sections, particularly those exposed to detergent extraction, it is possible to count the number of filaments in the rootlet. In different sections we counted 18–29 filaments making up the rootlet (Fig. 5). (The exact number is difficult to determine because some filaments, by being oriented somewhat obliquely, may be missed.) Therefore, of the >3,000 filaments in a stereocilium, only 18–29 penetrate into the cuticular plate. Each of these filaments measures ~65 \AA in diameter, whereas the filaments in the body of the stereocilium (often in the same section, e.g., Fig. 4) measure only 50 \AA in diameter. This difference in diameter between the two filaments is real and reproducible. In general, the filaments in the doughnut are only one filament layer thick. At the point of contact between the stereocilium and the cuticular plate, however, the doughnut can be more than one filament row in thickness (Fig. 5 *a* and *b*).

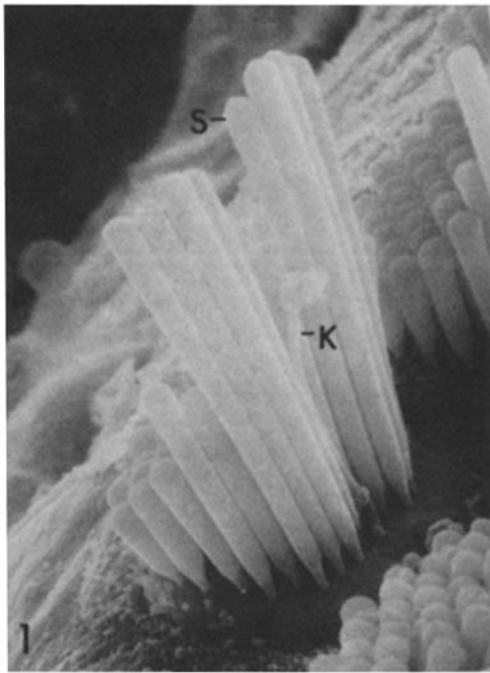


FIGURE 1 Scanning electron micrograph of the stereocilia (*S*) extending from a single hair cell. The single kinocilium (*K*) is indicated. The apical surface of the hair cells is flat as a result of the underlying cuticular plate. Peripheral to this flat surface are short microvilli, which extend from the supporting cells that surround and separate adjacent hair cells from their neighbors. $\times 5,000$.

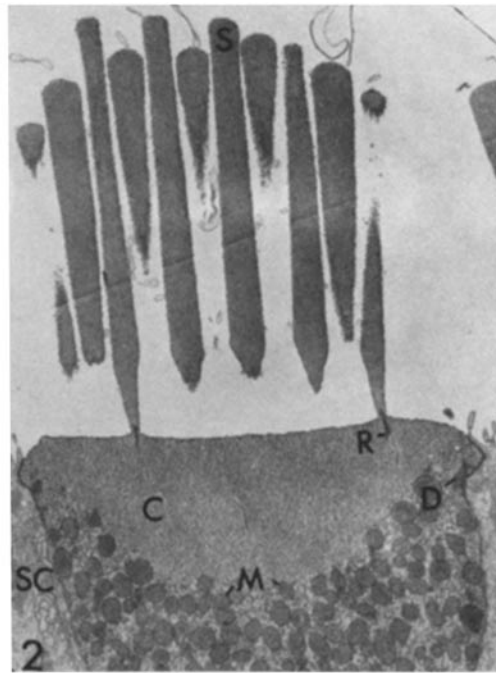


FIGURE 2 Thin section through the apical surface of a hair cell whose papilla was fixed with procedure *a*. On either side of the hair cell is the cytoplasm of a supporting cell (*SC*). Hair cells can be easily recognized by their stereocilia (*S*), the large cuticular plate (*C*) and the apical cytoplasm rich in mitochondria (*M*). The bowl-shaped cuticular plate does not extend all the way to the lateral margins of the cell. In this region there is frequently some dense material (*D*). The bases of each stereocilium enter the cuticular plate as a rootlet (*R*). $\times 8,200$.

Examination of Transverse Sections

Transverse sections of the stereocilia show a distinctive pattern in the organization of the filaments that is unusual and interesting. We find that the filaments show a considerable degree of order, yet they are not arranged in a regular lattice. Instead, the connections between neighboring filaments follow arcs that are stacked upon each other in rows to give a festooned pattern (Fig. 6) reminiscent of the pattern of folds in drapes that are pulled to the side of a window. We have examined numerous sections in which all the stereocilia from a single cell are cut in cross section. In these the direction and period of festooning are the same for all stereocilia from a single cell (Fig. 6). In sections in which the arrangement of the stereocilia appears disturbed, probably as the result of the dissection, both the period and the direction of festooning are different in adjacent stereocilia from the same cell. In sections such as these it is clear that the festooned pattern is not related to the direction of cutting, as can be determined by knife marks and chatter. Thus the pattern is clearly not a compression artifact.

We initially thought that perhaps the festooned pattern might be an artifact of fixation. Accordingly, we fixed the basilar papilla in a variety of media. Procedure *c*, consisting of both glutaraldehyde and osmium tetroxide simultaneously present, is particularly interesting because Flock et al. (10) demonstrated that with glutaraldehyde fixation alone the stereocilia did not remain rigid when bent with a fine needle. Also, simultaneous fixation tends to eliminate imperfections that occur with glutaraldehyde fixation alone (11). We also fixed papillae after detergent extraction in media of different com-

positions (procedures *d*, *f*, and *g*). In all cases, the festooned pattern of packing of the actin filaments was invariant.

The festooned pattern, then, represents some aspect of the organization of the filaments in the stereocilia. Because it often happens that neighboring stereocilia, even in adjacent cells, have similarly oriented festooning, it is of interest to relate the orientation of the pattern to the direction of sound propagation or, more specifically, to the movement of the endolymphatic fluid. This can be done by examining the position of the kinocilium relative to the stereocilia, because the movement of the stereocilia toward the kinocilium depolarizes the cell (12). When this was done, we found one case of the stereocilia bending perpendicular to the festooning and another of them bending parallel to it. Several others showed intermediate positions. Thus the festooned pattern cannot be related to the motions of the stereocilia caused by sound.

In sections where the arrangement of the stereocilia from a single cell is disturbed the variation in period of the festooned pattern can be considerable. For example, in one micrograph we measured periods of 450, 1,000, and 2,450 Å for adjacent stereocilia. These values are large relative to the center to center spacing of 90 Å between adjacent filaments (Fig. 6). Because large, variable periodicities are often associated with Moiré patterns that can arise from the superposition of detail at different levels within the specimen, we tilted some of the sections in the electron microscope. Tilt angles of up to 50° were tried with the tilt axis parallel to and perpendicular to the festooned pattern. No changes in the direction or period of the pattern were observed.

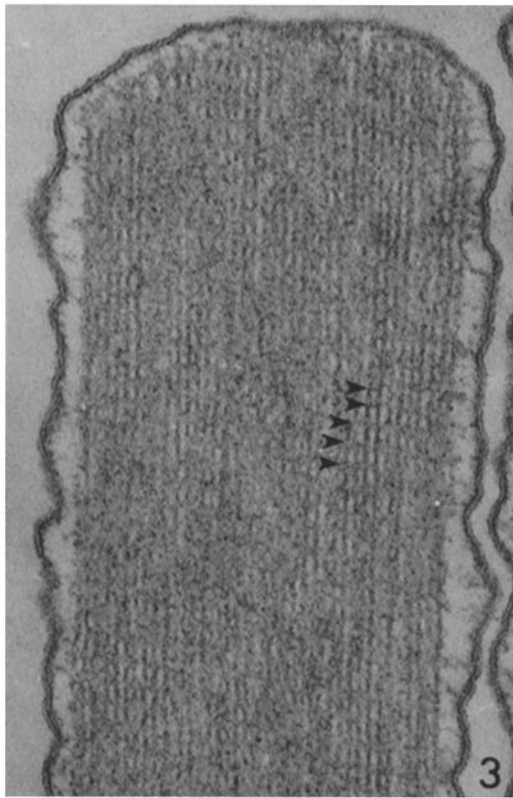


FIGURE 3 Thin section through the tip of a stereocilium fixed by procedure *c*. Note that there is a transverse periodicity running across the filaments. Some areas have been indicated by the arrows. This periodicity is best visualized by squinting along the surface of the micrograph perpendicular to the filaments. $\times 148,000$.

Changes in the pattern were observed, however, when we altered the thickness and direction of sectioning. First, we found that the festooned pattern present in a 230 Å (Fig. 7*a*) section can no longer be found in a serial section 450 Å in thickness (Fig. 7*b*). The section thickness could be accurately measured by halving the diameter of the thinnest section fold (see reference 25). In fact, the thickest section clearly showing festooning is 275 Å. Second, in succeeding serial sections, each ~ 130 Å in thickness, we have found that the festoons appear to shift laterally across the stereocilium (see the big arrows in Fig. 8). The period and direction of the motif are unchanged. Third, when the angle of a stereocilium relative to the knife is changed 10° , the period of festooning is changed from seven repeats (Fig. 9*a*) to nine repeats (Fig. 9*b*) on the same stereocilium.

Optical Diffraction Studies of Longitudinal Sections

In favorable longitudinal sections we see images reminiscent of an actin paracrystal (Fig. 3). The features expected to be seen in the diffraction patterns of the bundles and their relationship to the features in the image are shown schematically in Fig. 10.

When we took optical diffraction patterns of some of the longitudinal sections of stereocilia, we found prominent reflections lying on layer lines characteristic of actin (Fig. 11). The absolute spacings of the layer lines seem to vary with the fixation procedure and are substantially less than those of native actin: for example, with procedure *b* we observe spacings

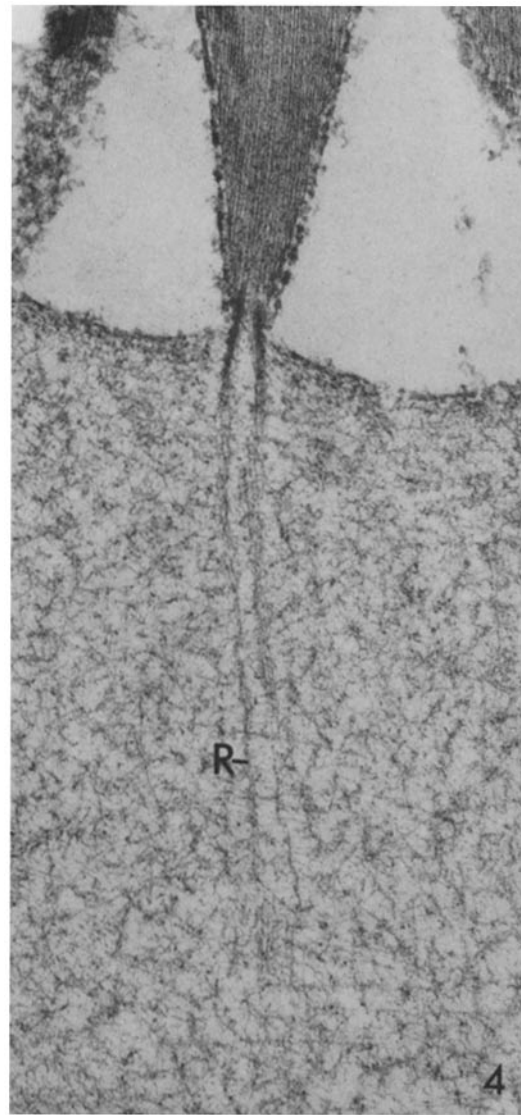


FIGURE 4 Thin section cut through the basal end of a stereocilium and the cuticular plate. Of interest is the tubular rootlet (*R*) composed of filaments that penetrate through the filaments in the cuticular plate. This papilla was extracted with the detergent, Triton X-100, then fixed by procedure *d*. $\times 60,000$.

of 347, 55.3, and 47.5 Å and with procedure *c* we measure values of 246, 46.7, and 34.2 Å. Although such values are less than those expected for pure actin, 375, 59, and 51 Å, there is no reason to suspect that this shrinkage is not just an artifact of the preparative procedure for microscopy. Reedy (25) has also found 10–20% shrinkage in the fixing and embedding of muscle for microscopy. From the ratio of the spacing of the $1/375$ and $1/59$ Å layer lines, a value that is not sensitive to shrinkage, we can determine the screw parameter of the filaments, which lies in the range found for different actins from both muscle and nonmuscle sources. More specifically, in the actin filaments in the stereocilia there are 2.159 actin units per turn, which falls between the value of 2.167 for rabbit skeletal muscle actin (17) and 2.154 for actin from *Limulus* sperm (4). The value of 2.159 actin units per turn tells us that the actin filaments in the ear are not unusually tightly or loosely twisted, a measurement that is important because in *Limulus* sperm a change in the twist of the actin helix is closely correlated with the movement of that system (5).

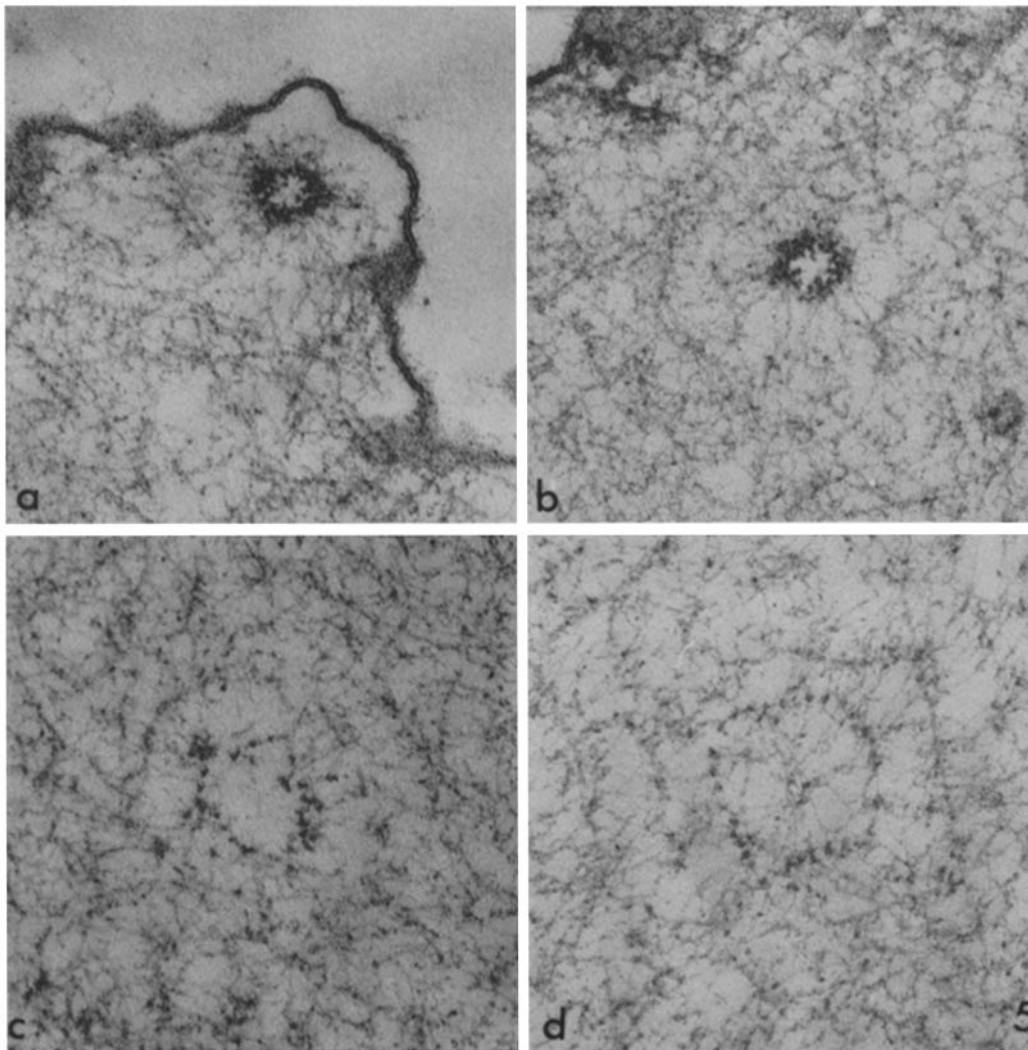


FIGURE 5 Transverse sections through the rootlet at progressively deeper levels in the cuticular plate. Individual filaments in the rootlet can be identified and counted. The rootlet appears as a cone that increases in diameter the farther it penetrates into the cuticular plate. Extending peripherally from the rootlet and also extending across the rootlet in *c* and *d* are fine filaments, 30 Å in diameter, that interconnect the rootlet filaments. Fixation is by procedure *c*. $\times 154,000$.

The distance between row lines (a measurement of the center to center spacing of actin filaments (see Fig. 11) is $1/89 \text{ \AA}^{-1}$. The interfilament spacing, therefore, is $89(2/\sqrt{3})\text{\AA} = 103 \text{ \AA}$.

There is an additional feature to the diffraction pattern of stereocilia that tells us about the relationship between neighboring actin filaments. The row lines are tilted off the vertical by 10° (Fig. 11). Thus the crossover points of adjacent filaments are almost, but not quite, in register; they are shifted axially by $103 \text{ \AA}(\tan 10^\circ) = 18 \text{ \AA}$ relative to the crossover points of the adjacent actin helices. This measurement is accurate to $\pm 5 \text{ \AA}$.

Fine Filaments Associated with the Rootlet and the Cuticular Plate

An examination of thin sections cut through the cuticular plate using fixation procedures *b*, *c*, and *d* reveals that it is composed of what appears to be a network of fine filaments traveling in all directions. The filaments vary in thickness from 30–60 Å. Careful scrutiny of the rootlet filaments that extend from the stereocilia reveals that these filaments are interconnected by fine, 30 Å filaments (Fig. 5*d*). In longitudinal section

these fine filaments have a ladderlike appearance. In transverse sections through the rootlet, we frequently see that the rootlet filaments are connected together in a spokelike arrangement reminiscent of a wagon wheel (Fig. 5*d*). These spokes are composed of the 30 Å filaments that are often not well ordered. In transverse sections through the compact rootlet in detergent-extracted papillae at the junction with the stereocilium, we find fine filaments (30 Å) that extend from the rootlet radially outward toward where the membrane should be (Fig. 12). We presume that these fine filaments stabilize the connection between the membrane and this part of the rootlet. The images of the 30 Å filaments are particularly clear in papillae fixed simultaneously with glutaraldehyde and osmium tetroxide (procedure *c*) (Fig. 5), or fixed after detergent extraction (procedures *d* and *e*) (Fig. 12).

Other parts of the cuticular plate also show order that consists of parallel arrays of filaments each $\sim 60 \text{ \AA}$ in diameter interconnected by fine, 30 Å filaments. These arrays tend to be found at the lateral and basal margins of the cuticular plate and are not oriented with respect to the rootlet filaments. In certain cuticular plates they can be very prominent. Microtu-

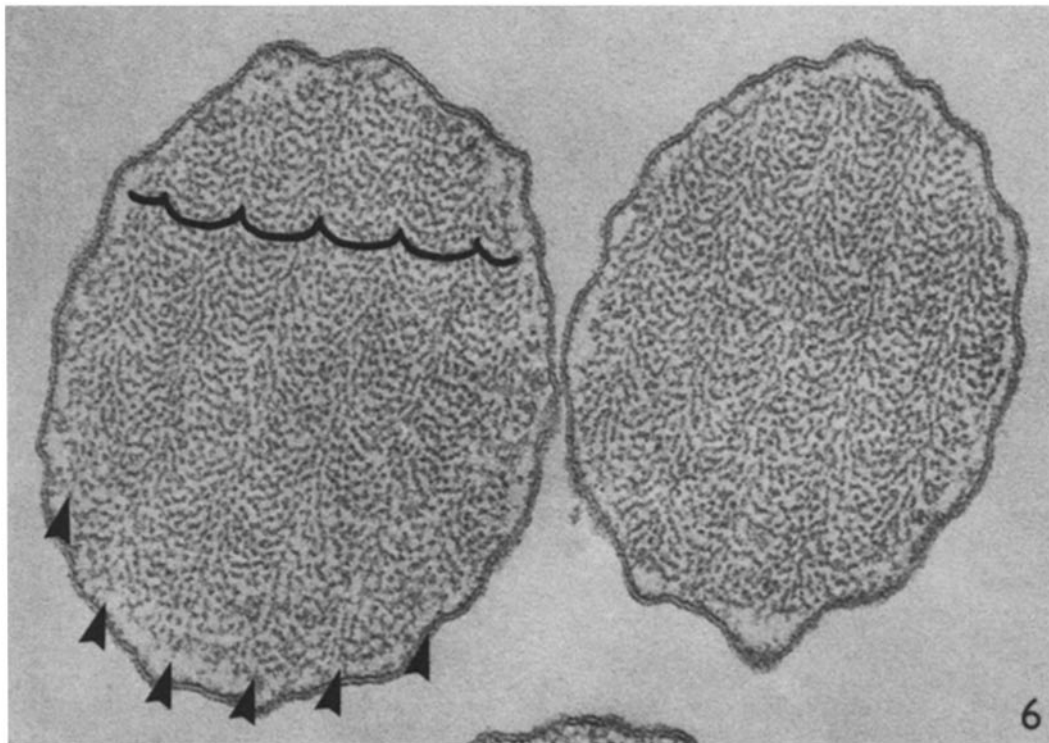


FIGURE 6 Thin transverse sections through two stereocilia cut midway along their lengths. The filaments are not hexagonally packed, but are arranged to produce a festooned pattern (see tracing). The arrows indicate the period of festooning. Note that the pattern of adjacent stereocilia is identical. Fixation is by procedure *b*. $\times 170,000$.

bules are often found at the margins (both lateral and basal) of the cuticular plate. Most frequently, 60 Å filaments run parallel to the microtubules, being separated by ~ 100 Å from them. Tiny cross-connections between these two types of fibrous structures are found.

Decoration of the Actin Filaments with Myosin S1

The filaments within the stereocilia decorate with S1 to give the characteristic arrowhead appearance, as was predicted from the results of Flock and Cheung (9) on the hair cells of the vestibular apparatus (equilibrium organ). Unlike the results of Flock and Cheung (9), under our conditions the decoration induces the filaments in the stereocilia to splay apart and thus the polarity of most, if not all, of the filaments within a single section can be readily determined (Fig. 13). We have looked at many images similar to that illustrated in Fig. 13 and invariably all the filaments decorate and, interestingly, the arrowheads on all these filaments point toward the cell center. Thus the polarity of all the filaments in the stereocilia is the same. The filaments in the rootlet also decorate and the polarity is identical to that of the filaments in the stereocilia; that is, the arrowheads point towards the cell center (Fig. 14). These filaments, then, would presumably extend from the rootlet to the tip of the distal end of the stereocilia.

In some preparations the membrane limiting the tapering portion of the filament bundle remains and we can demonstrate conclusively that the peripherally located filaments in the bundle terminate on or very near the membrane (Fig. 13). From these images, then, there is no evidence that the peripheral filaments twist or coil over one another but, rather, they

extend straight from the tip of the stereocilium to their termination point. In addition, it appears that the filaments in the rootlet that begin in the cuticular plate extend up the middle of the stereocilium.

The majority of the filaments in the cuticular plate also decorate, indicating that they are actin; yet, unlike the rootlet filaments, the bulk appear to be randomly oriented (Fig. 14). However, there are also a number of 30 Å filaments that do not decorate (Fig. 14). Because all the filaments in the stereocilia decorate, as is true of all their extensions in the rootlet and the actin filaments in the cuticular plate, it is unlikely that these fine, 30 Å filaments did not decorate because of a lack of S1. Instead these filaments constitute a second population of filaments that are not actin, a conclusion strengthened by the fact that they are too slender to be actin. These 30 Å filaments seem to be confined to the cuticular plate, as they are rarely seen amongst the actin filaments in the stereocilia. In general these 30 Å filaments connect actin filaments together. Some appear to extend towards where the membrane is, or would be.

S1 decoration also shows us that the cuticular plate is isolated from the lateral surface of the cell. The cuticular plate filaments do not reach out towards the membrane at the apicolateral surface of the cell. Instead, there is another set of actin filaments in the hair cells (Fig. 15). This population penetrates into a dense filamentous material that at foci is attached to the lateral surface of the cell. It is noteworthy that there is a corresponding dense filamentous material in the supporting cells that attach to the lateral surface of the supporting cell membrane opposite the insertion of the dense material in the hair cell (Figs. 2 and 15). This second population of filaments (inserted into the dense material) extends into the cytoplasm in all directions, but is easily differentiated from the filaments making up the cutic-

ular plate, although both decorate. The result of having two populations of filaments in the apical cytoplasm is that the lateral surfaces of the cell are stabilized, as is the central region (cuticular plate), but the cuticular plate is not physically connected to the lateral filaments. Movement of the plate, then, would not distort the lateral surfaces of the cell except by fluid coupling.

Incubation of Demembrated Papillae with Media Lacking Divalent Cations or Containing Ca^{++} , Mg^{++} , and ATP

Longitudinal and transverse sections through the stereocilia and the cuticular plate were examined from cells demembra-

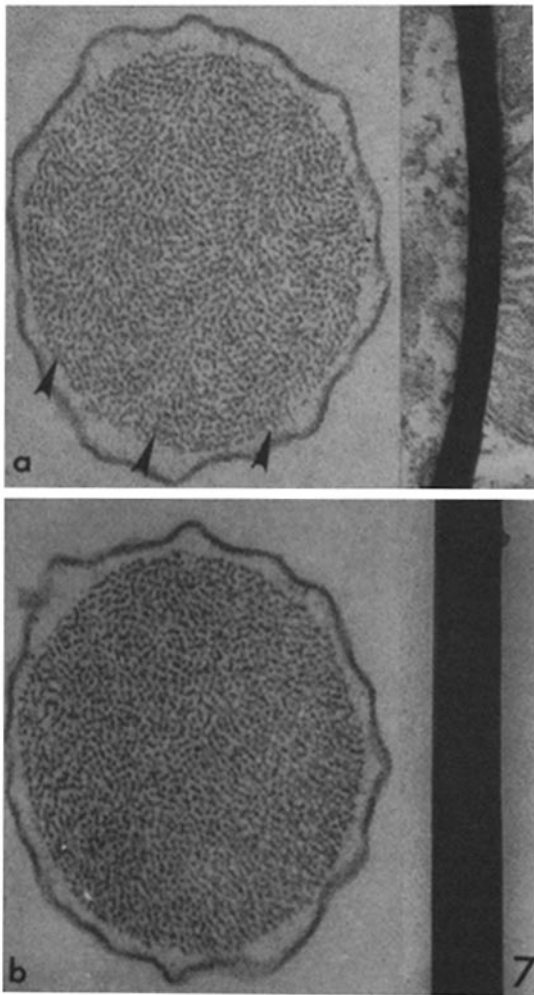
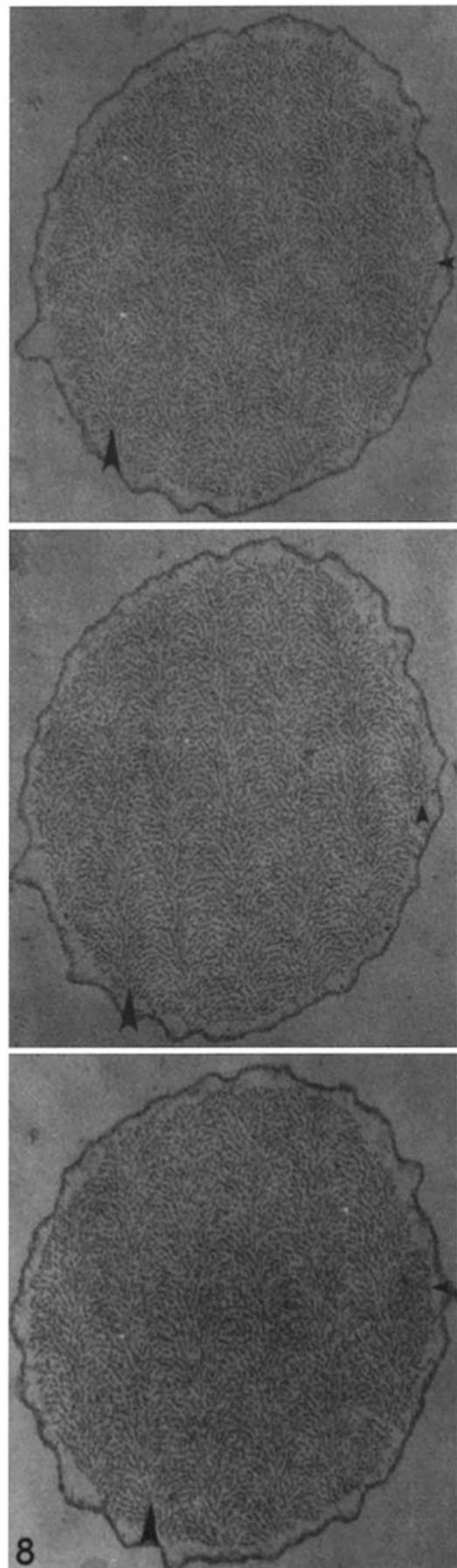


FIGURE 7 Serial sections cut through the same stereocilium. The section thickness can be measured after the method of Reedy (25) in which the thinnest fold will be twice the thickness of the section. Note that *a* is 230 Å in thickness, yet *b* is 450 Å in thickness. Of interest is that in thin sections (*a*) the festooning is obvious (see arrows), whereas in thicker sections (*b*) the festooning disappears. $\times 100,000$.

FIGURE 8 Three serial sections of the same stereocilium. By careful examination of the position of the large vertical arrow on these three sections, it is clear that in serial sections the festooned pattern is shifting horizontally. Another way to see this is to look at the right edge (small arrows). Notice that the filaments are elongated horizontally in *a*, vertically in *b*, and horizontally again in *c*. $\times 92,000$.



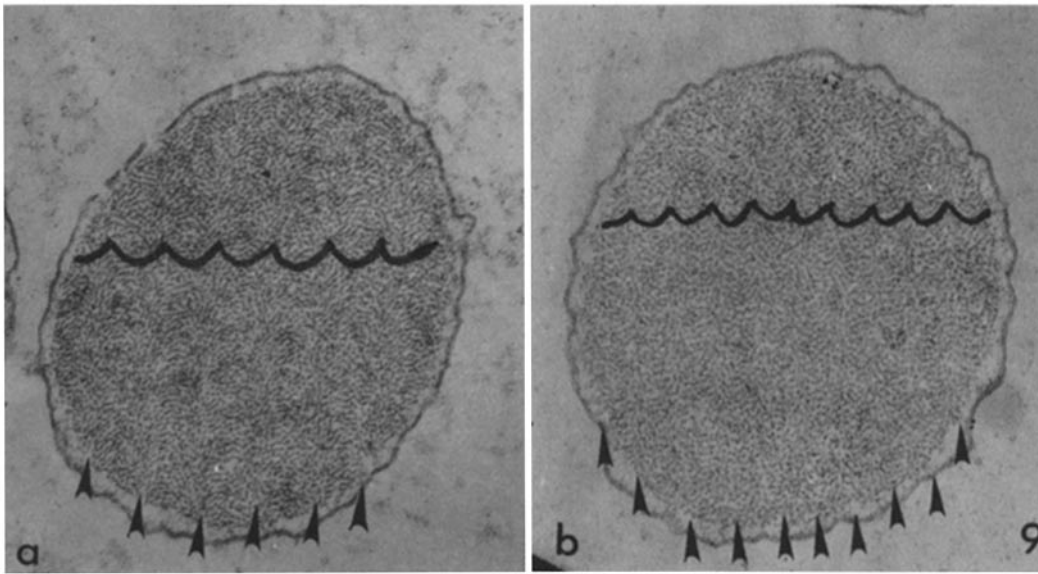


FIGURE 9 Thin sections of the same stereocilium. In *a*, we see seven festoons, as illustrated by the arrows and the scalloped ink line. In *b*, where the block has been turned 10° away from the knife, we can see nine festoons. $\times 78,000$.

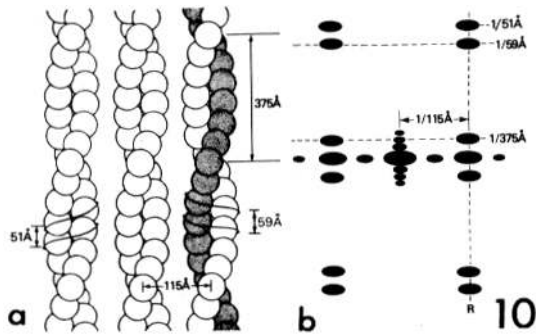


FIGURE 10 (a) A diagram of a paracrystalline array of actinlike filaments in which the crossover points of the helices are in register. The lines indicate one of the prominent helical families, one having a pitch of 59 \AA , another of 51 \AA , and the third of 375 \AA is indicated by the stippling. Adjacent filaments are separated by 115 \AA . (b) A diagram of the expected diffraction pattern of the array illustrated in *a*. The pattern consists of a series of horizontal layer lines that arise from the helical symmetry of the actin. These layer lines occur at spacings of $1/375$, $1/59$, and $1/51 \text{ \AA}^{-1}$. The strong spots on the different layers are lined up vertically in columns called row lines. The row lines arise from the paracrystalline arrangement of the adjacent filaments. Spacing of the row lines is $1/115 \text{ \AA}^{-1}$.

nated and then incubated in a solution containing EGTA and EDTA to chelate out all the divalent cations (procedure *f*). The packing of the filaments into the paracrystalline-festooned appearance was not altered (Fig. 16). This indicates that the bridges holding adjacent actin filaments together do not rely on Mg^{++} or Ca^{++} directly or indirectly and that the paracrystalline packing cannot be attributable to Mg^{++} . Also the packing and relationship of the filaments relative to the cuticular plate did not change.

We also demembrated papillae in a solution containing Ca^{++} and Mg^{++} -ATP (procedure *h*), or, in another experiment, first demembrated and then incubated the papillae in Ca^{++} and Mg^{++} -ATP (procedure *g*). Unlike the intestinal microvilli, the stereocilia did not move into the cuticular plate. In fact, this procedure was repeated twice more, using new papillae, with identical results; furthermore, we could not see any dif-

ferences in the cuticular plate. In addition, there was no change in the packing of the actin filaments in transverse or longitudinal sections, the image appearing identical to Fig. 16.

DISCUSSION

The new information presented in this report is the following: first, we have described the polarity of all the actin filaments in the stereocilia, in their rootlets, in the cuticular plate, and attached to the lateral membranes. Second, we have described a population of 30 \AA filaments in the cuticular plate that do not decorate with S1 and that appear to function in cross-linking the filaments to each other and to the membrane. Third, we have examined the packing of the filaments in the stereocilia and have found that they are aligned into paracrystalline order with the crossover points in near-perfect register. Fourth, we have shown that the filaments in transverse section show a festooned pattern that we interpret as indicating that the actin filaments are bridged together at frequent and rather precisely dictated intervals, although, unlike other paracrystals of actin, the filaments are not hexagonally packed. Fifth, the application of media deficient in divalent cations or containing magnesium and/or calcium and ATP does not change the packing of the actin filaments.

Flock and Cheung (9) have suggested a homology between the stereocilia in the ear and the brush border of intestinal epithelial cells. In the discussion that follows we will first show, by a comparison of these two systems, that they are very different and conclude that they do not act in an analogous fashion: the microvillus has a design that allows it to shorten, whereas the stereocilia are designed to pivot. We will then describe what might be the consequences of the packing of the actin filaments in the stereocilia.

Evidence against Functional Homology between Stereocilia in the Ear and Microvilli of Intestinal Epithelial Cells

There are two obvious similarities between the microvilli and the stereocilia: (a) both contain actin filaments and (b) all

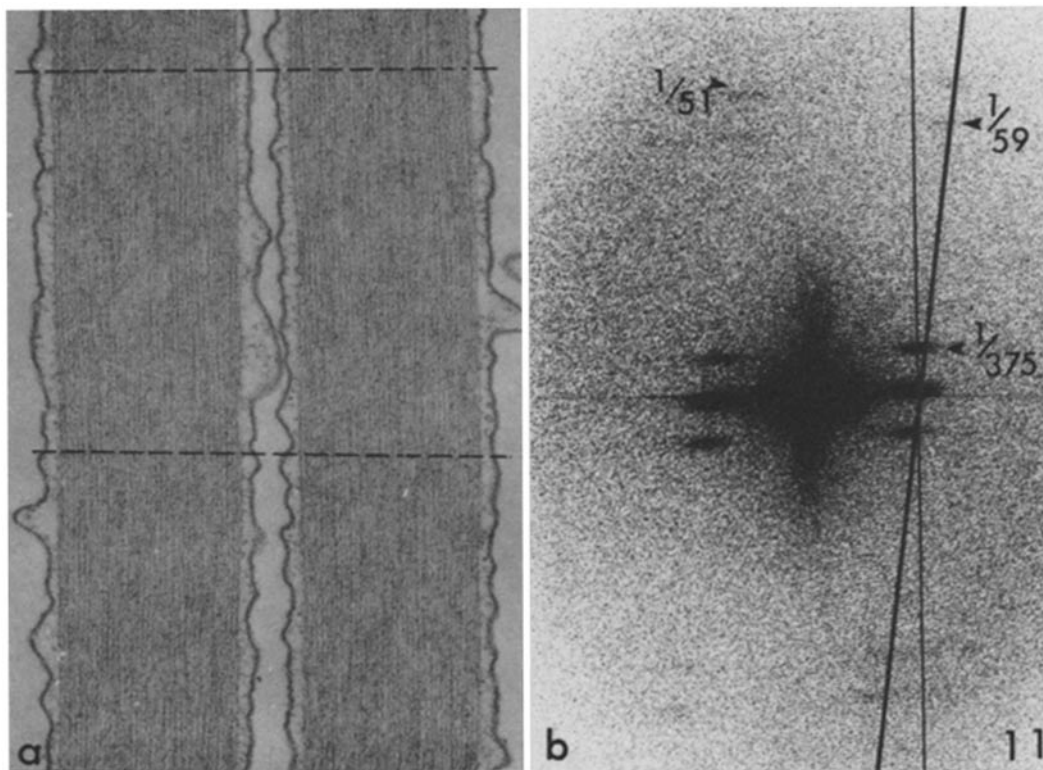


FIGURE 11 (a) Longitudinal section through two stereocilia fixed according to procedure *b*. The diffraction pattern of the area outlined by the dotted lines is shown in *b*. Note that there are prominent reflections on the $1/59$, $1/51$, and $1/375$ Å lines, but because of shrinkage the measured values are smaller. The row lines at $1/89$ Å⁻¹ are tilted off the vertical by 10° as indicated by the solid lines of differing thickness. (a) × 73,000.

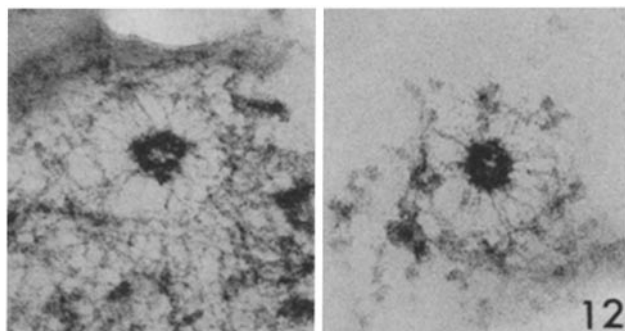


FIGURE 12 Cross sections through the bases of two stereocilia at the point where the stereocilia make contact with the plasma membrane covering the cuticular plate. Of interest are the 30-Å filaments that extend from the rootlet towards where the membrane would be located. These preparations were first extracted with detergent, then fixed (procedure *d*). × 146,000.

the actin filaments have the same polarity. Yet, the design of these two systems is very different, which must relate to differences in their functions.

ACTIN FILAMENT-MEMBRANE ASSOCIATION: In the stereocilia of the ear, the lateral separation of the filament bundle from the membrane is 100 Å. In some places the separation is greater, but this appears to be the result of improper fixation. The close association of filaments and membranes is presumably the mechanical link responsible for opening ion channels.

The filament core bundle in the microvilli of the intestine, in contrast, is separated from the membrane by ~200–300 Å (30).

Presumably this space permits diffusion of absorbed fatty acids, sugars, etc. (20).

THE ORGANIZATION AND FUNCTION OF THE ROOTLET IN BOTH SYSTEMS—THE ROLE OF THE 30 Å FILAMENTS: In sections cut through the cuticular plate, we are struck by an enormous number of 30 Å filaments that are not actin filaments. This is particularly obvious in preparations decorated with S1. The rootlet system in the cuticular plate acts like the roots of a tree that spread underground, splaying laterally, to anchor the tree. These roots intertwine and are then cross-linked by the 30 Å filaments to other underground roots (the enormous number of actin filaments in the cuticular plate). In contrast, in the brush border of intestinal epithelial cells, the bulk of the filaments in the terminal web are the core filaments extending from the microvilli. The rootlets, instead of splaying outward, resemble the single tap root of a tree. Begg et al. (2) have described a population of 30 Å filaments in the brush border similar in morphology to those described here in the hair cells, although the organization is different; their 30 Å filaments, instead of connecting filaments within a bundle to those in the terminal web, are only found at the periphery of the core filament bundle. Thus the rootlet filaments of the stereocilia are designed to be firmly anchored in the cuticular plate allowing the structure to pivot as a rigid lever at the point of connection with the cuticular plate, as has been observed by Flock et al. (10).

THE APICAL CELL SURFACE—CUTICULAR PLATE VS. TERMINAL WEB: In both the brush border and in the hair cells there is a population of filaments at the level of the zonula adherens attached to the lateral margins of the cell (13; Tilney, unpublished observations). In the brush border the chemical

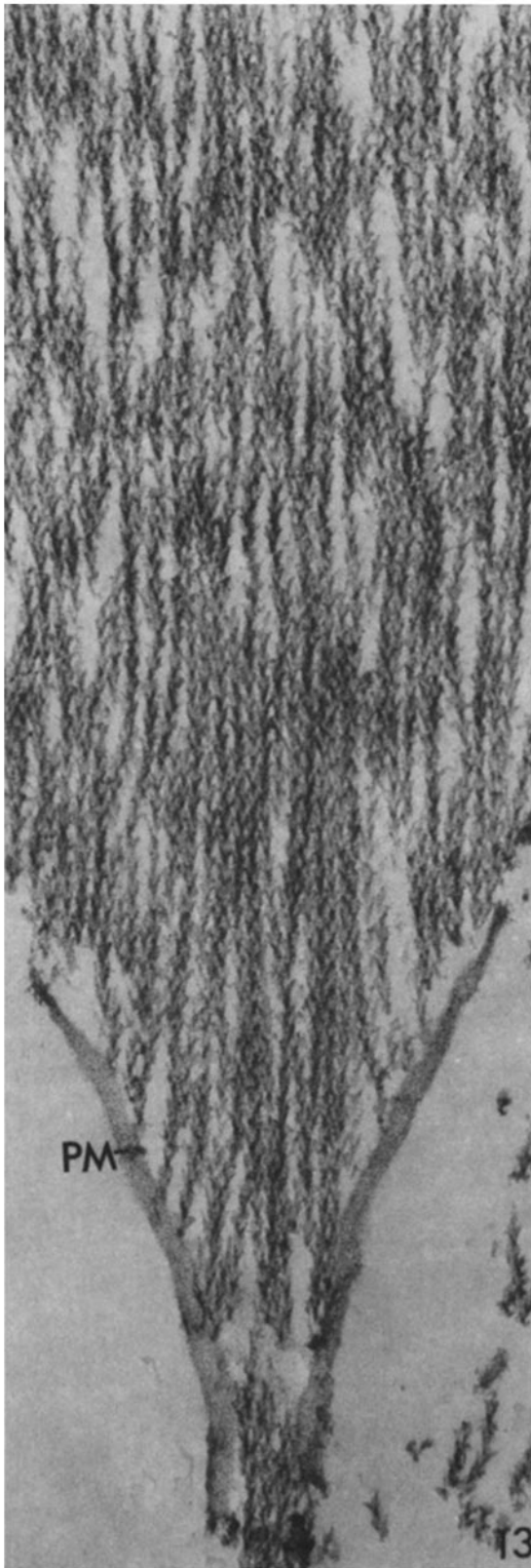


FIGURE 13 Thin section through the basal end of a stereocilium that was demembrated and then decorated with subfragment 1 of myosin (S1). Note that all the filaments are decorated and the arrowheads all point towards the cuticular plate. A fragment of the membrane (PM) limiting the basal end of the stereocilium remains. It illustrates how the filaments terminate in an ordered way as the stereocilium tapers. $\times 102,000$.

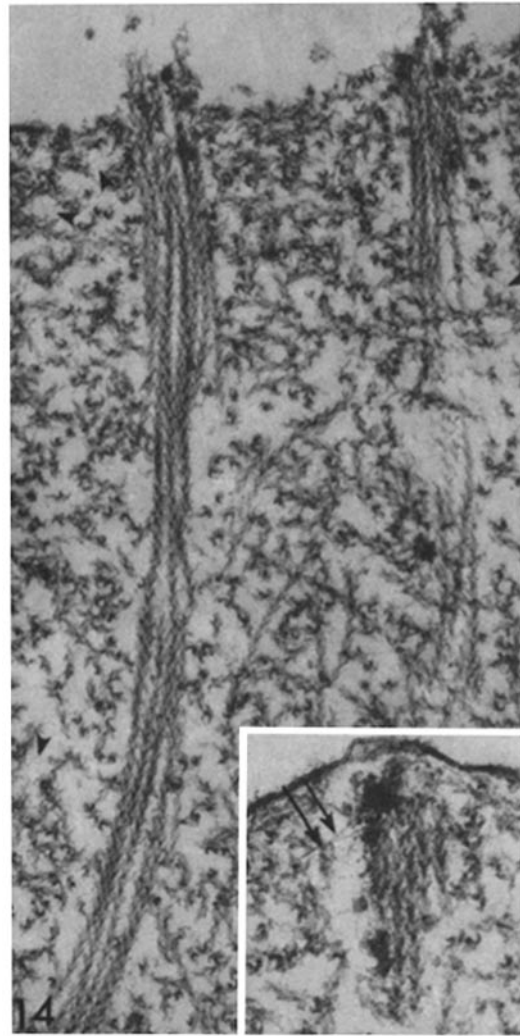


FIGURE 14 Section through the cuticular plate from a papilla demembrated and then decorated with S1. It is of interest that the majority of the filaments in the cuticular plate are actin filaments; their polarity is random. The rootlet is comprised of actin filaments even in the region where the dense material surrounds the rootlet filaments. These filaments have the same polarity as the actin filaments in the stereocilia with which they are continuous. The arrows indicate a second set of fine filaments that do not decorate and that appear in positions similar to the 30-Å filaments illustrated in Figs. 5 and 12. $\times 72,000$. Inset, higher magnification of the region near the membrane. Of note are the 30-Å filaments attached to the rootlet (see double arrow). $\times 117,000$.

nature of these filaments is still controversial, but Rodewald et al. (26) have demonstrated that addition of ATP and Mg^{++} or Ca^{++} leads to a compression or reduction in size of the apical cell surface. The impressive feature in this system is that the apical cell surface of the epithelial sheet remains intact when detergent extracted (20), the apicolateral surface behaving as a unit, not as isolated cells. Thus the filaments attached to the lateral surfaces of the cell are in direct continuity with the terminal web (13). The only break in this sheet is seen when one encounters goblet cells. In the hair cells, in contrast, the filaments that extend from the lateral margins of the hair cell are not in direct continuity with the actin filaments of the cuticular plate, but rather are separated by a thin layer of cytoplasm. This fact was established in S1-decorated cells after detergent extraction. This arrangement of filaments structurally

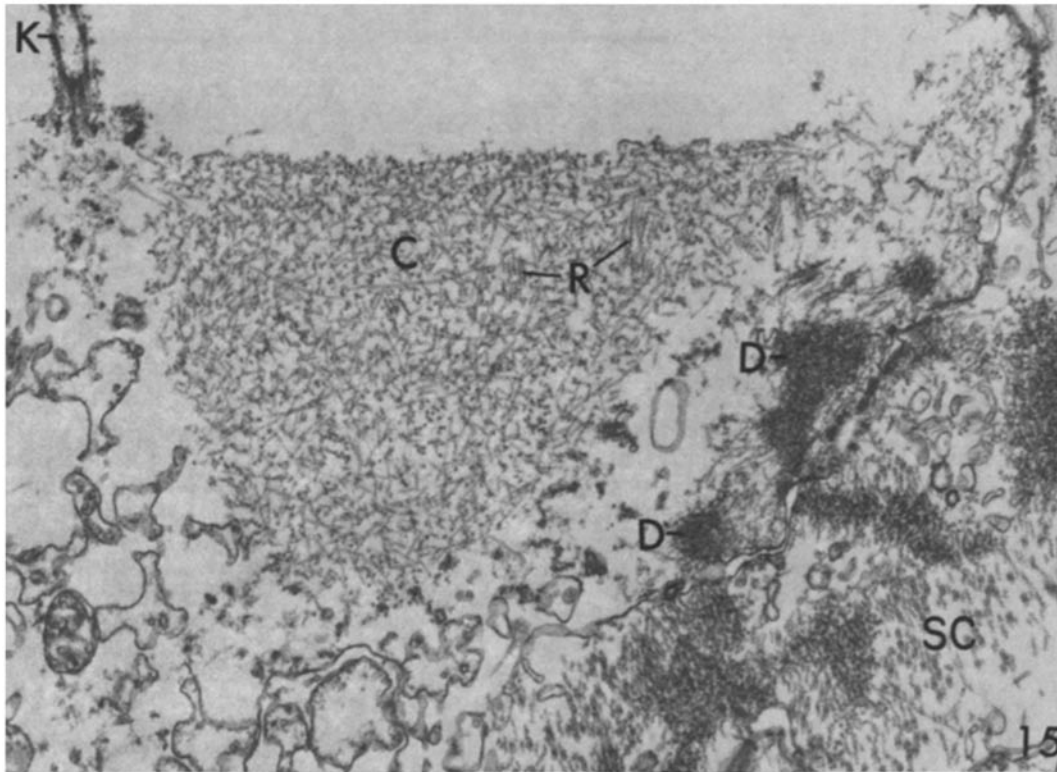


FIGURE 15 Thin section through the apical end of a hair cell from a papilla demembrated and decorated with S1. A portion of a supporting cell (SC) is seen on the right. Note that the cuticular plate (C) with its rootlet (R) is separated from the lateral surface of the cell. Near this surface is some dense material (D) from which are inserted a number of decorated actin filaments that constitute a second set, as they do not make contact with the cuticular plate. Dense masses of material and associated actin filaments are present in the supporting cell. The basal end of the kinocilium (K) is also illustrated: it is not inserted into the cuticular plate. $\times 9,200$.

isolates the cuticular plate from the lateral margins of the cell.

Also in the ear, in contrast to the intestine, there is a second population of cells, the supporting cells, which contain within their apical cytoplasm large bundles of actin filaments attached to the lateral membrane surfaces. Often the bundles of filaments in a supporting cell interact with a region of the membrane between the supporting cell and the hair cell where there is a corresponding bundle of filaments attached to the hair cell membrane. The filaments in the supporting cell interact to form a ring of fibrous elements around each hair cell. The supporting cells also contain a large population of microtubules parallel to the long axis of the cell; presumably, these tubular elements act to stabilize the long axis of the cell. Thus the sensory epithelium of the ear seems to be designed to allow the cuticular plate to float relatively unattached, like a cork in liquid, yet the integrity of the epithelium is maintained largely by the two types of fibrous elements in the supporting cells and in the apicolateral portion of the hair cells. In essence, looking down on the epithelium, one gets the impression of Swiss cheese with the holes being the spaces within which the cuticular plate and its associated stereocilia float.

STEREOCILIA ARE DESIGNED TO PIVOT RATHER THAN SHORTEN: The stereocilia of the ear taper, having some 3,000 filaments at the tip but only 18–29 at the base where the stereocilium enters the cell body. This taper is not gradual, but occurs largely at the base so that the stereocilium resembles a sharpened pencil. If the stereocilium were designed to shorten, we would not expect to see such tapering at the base where the force would be generated.

In contrast, the microvilli in the intestinal brush border, which can shorten *in vitro* (18), have a constant, small number (20–30) of filaments along the whole length. When the same conditions that cause a shortening of the microvillus are applied to the stereocilium, no shortening occurs.

Thus, the striking differences in design between these two systems, and the failure of calcium and ATP to induce shortening of the stereocilia, lead us to conclude that the stereocilia are designed to behave as levers, not to shorten.

The Packing of Actin Filaments in the Stereocilia

IMPLICATIONS OF THE OPTICAL DIFFRACTION PATTERNS: We will begin with a brief discussion of what can be learned about the packing of actin filaments from the optical diffraction patterns. Actin often forms bundles *in vivo* and *in vitro* in which the crossover points of neighboring filaments are exactly in register. A portion of such an arrangement is shown schematically in Fig. 10. Each filament consists of a family of helices as a result of the arrangement of subunits. One helix of pitch 59 Å can be drawn through all the subunits of the filaments. In one turn of this helix, which is left-handed, there are slightly over two subunits. Features such as grooves or ridges that parallel this helix give rise to the corresponding (horizontal) $1/59 \text{ \AA}^{-1}$ layer line in the optical diffraction pattern shown schematically in Fig. 10*b*. There is a second helix, in this case right-handed, which also goes through the subunits; this helix has a pitch of 51 Å and gives rise to a $1/51 \text{ \AA}^{-1}$ layer line in the optical diffraction pattern. There is a third helix,

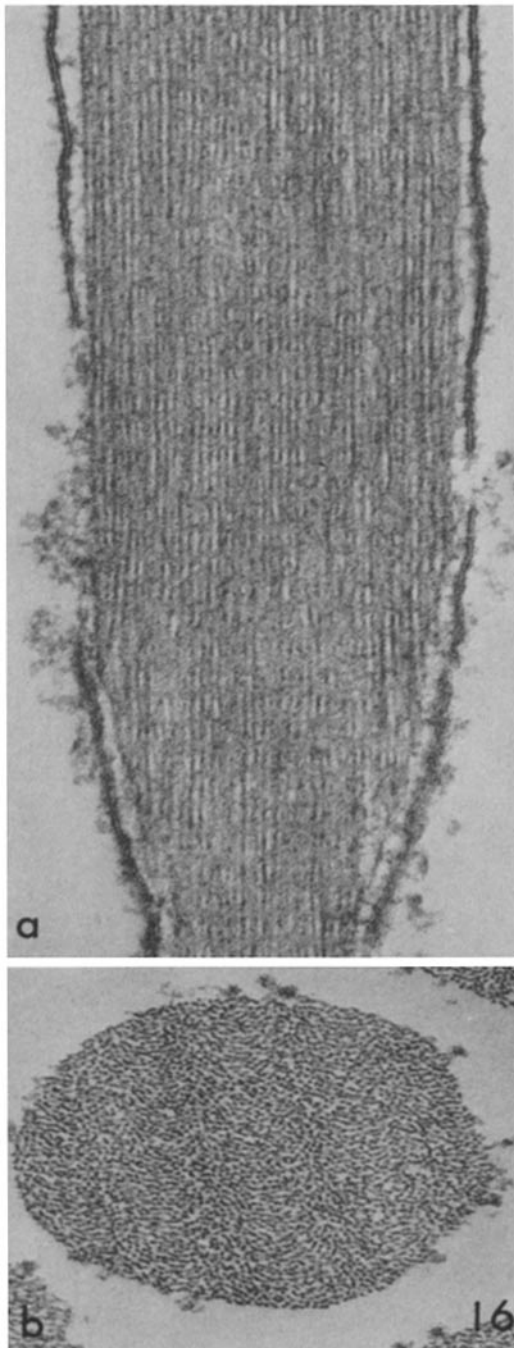


FIGURE 16 Longitudinal and transverse sections through stereocilia that were demembrated, incubated in 5 mM EGTA and 5 mM EDTA, and then fixed (procedure e). Note that the filaments have the same packing as in untreated stereocilia in both longitudinal (a) and transverse (b) sections. (a) $\times 140,000$, (b) $\times 103,000$.

actually a pair of right-handed helices, having a pitch of 375 Å; this has a corresponding layer line of $1/375 \text{ \AA}^{-1}$. The ratio of the pitches of the 59 Å and the 375 Å helices determines exactly the number of units per turn (U/t) of the single helix ($U/t = 2 + 59/375 = 2.157$). Pitches vary for different actins, but U/t has always been found to lie between 2.15 and 2.17. Usually in images of arrays of filaments the crossover points or narrowest aspects of the filaments are found in register as in Fig. 10a. In diffraction patterns this arrangement has the following consequences: the strongest reflections or spots are

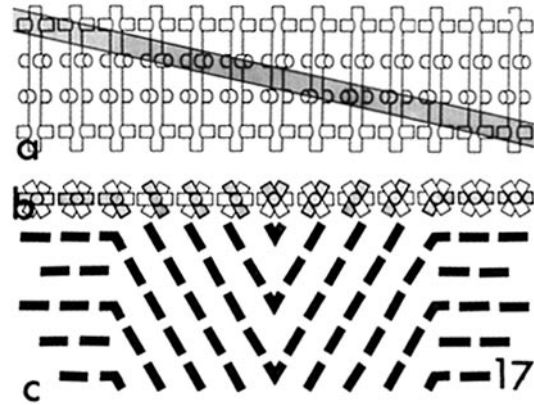


FIGURE 17 Model of the way in which large-scale periodicities can arise. (a) A row of a hexagonal array of hypothetical filaments with helically arranged arms that connect neighboring filaments. An imaginary oblique, thin section of this structure is indicated by the stippled area. (b) An end-on view of the row of filaments in an oblique section taken through the array of filaments illustrated in a (the stippled portion of a). The stippled portions denote those parts of the filaments and bridges included in the section. The unstippled, absent portions are included to provide a frame of reference. Notice that as the section rises from right to left the direction of the stippled arms that are in the section changes: at the right they are at 3 and 9 o'clock (i.e., horizontal); then farther to the left they switch to 11 and 5 o'clock; still farther on they again switch to 7 and 1 o'clock; and finally at the right edge, return to 9 and 3 o'clock. (c) A drawing of the pattern expected for a two-dimensional array of filaments. Just that portion of the filament and its arms included in the section are shown. Note that the pattern is festoonlike and can be seen to repeat after 12 filaments.

confined to the intersection of the horizontal layer lines (a demand of the helical symmetry) and the vertical row lines (a demand of an array of filaments). In the array illustrated in Fig. 10, the separation of adjacent filaments as seen in projections is 115 Å. The spacing between filaments in the bundle is $115(2/\sqrt{3}) = 133 \text{ \AA}$. The position of the row line is, therefore, $1/115 \text{ \AA}^{-1}$ in the diffraction pattern. If the row line is exactly vertical, as shown in Fig. 10, the crossover points are exactly in register. If the row line makes an angle of θ off the vertical, then neighboring crossover points are shifted vertically by an amount of $d \tan \theta$, where d is the spacing between filaments. If the filaments are parallel to each other, but the crossover points of neighboring filaments are not in register, then, on all layer lines except the equator, the strong spots that give rise to the row lines would not be present. Instead, diffracted light would occur all along the layer lines, not just at one point.

The observed transform (Fig. 11) has the features we have described: a horizontal set of layer lines indicating a typical actin structure having 2.159 U/t and a nearly vertical set of row lines showing that adjacent actin filaments have their crossover points in near-perfect register.

The filament separation for the stereocilia measured from the row lines is 100 Å, about twice the value measured for paracrystals of purified muscle actin, 60 Å (17). Such a large value suggests the presence of a cross-bridging protein between actin filaments whose presence results in a much larger spacing than is found in the Mg^{++} paracrystals containing only actin.

A similar large spacing (90 Å) is observed in "needles" (paracrystals) of actin from sea urchin oocytes (14), which contain actin held together by cross-bridges of 55,000-dalton proteins. In the sea urchin material, DeRosier et al. (4) have

shown that the cross-bridges give rise to a 110-Å meridional reflection that is not seen in paracrystalline specimens of pure actin. Cross-bridges have also been observed by Spudich and Amos (27) in the microvilli of sea urchin oocytes. In the microvilli, the presence of cross-bridges is reflected in the meridional reflection at 130 Å. Thus such a meridional reflection coupled with a large filament separation is strong evidence of the presence of cross-bridging material. We have examined many preparations of the stereocilia for a meridional spot and have been unsuccessful in finding one. On the other hand, in the stereocilia of the bird cochlea we find a meridional spot at a spacing of 125 Å (Tilney and DeRosier, unpublished observations), which is essentially the same value as was measured for cross-bridged bundles of actin filaments in other systems. However, in bird stereocilia, in microvilli, in *Mytilus* sperm, and in needles (paracrystals) from sea urchin oocytes, the actin filaments are packed hexagonally, not as in the lizard stereocilia. The lack of a meridional spot in lizard stereocilia, then, is attributable to the difference between the packing in this system and that in other systems, as will be the subject of a forthcoming publication.

Thus our optical diffraction results tell us that the filaments in the stereocilia (*a*) are packed with paracrystalline order (an observation that cannot be made rigorously by merely looking at select areas of certain micrographs), (*b*) have the crossover points of the adjacent actin filaments shifted 20 Å relative to those of their neighbors, (*c*) have a structure and number of units per turn similar to that of other actins, and (*d*) are probably held together by cross-bridges.

WHAT GIVES RISE TO THE FESTOONING: We think that the festooned pattern arises from the helical arrangement of cross-bridges that connect adjacent filaments. A similar mechanism has been invoked to explain patterns seen in thin sections of insect flight muscle (25). Fortunately, our hypothesis is readily testable. Our idea is perhaps most easily visualized by the model in Fig. 17, in which we see a bundle of filaments with three sets of cross-bridges extending from each of them. If we were to cut a thin section through this bundle, as illustrated by the stippled area, we would first cut through the lower set of cross-bridges on the leftmost filaments, then the second set on the middle filaments, and finally the top set on the rightmost filaments. If we were to pick up this section, turn it on its face and look down on it as one would look at a section in the electron microscope, we would see the image indicated by the stippled area in Fig. 17*b*. This stippled area shows the bridges and cross sections of filaments included in that thin section. Other bridges that would not be included in that particular section are also indicated, but they are not stippled. Looking down on the section, then, we would see filaments as indicated by dashed lines in Fig. 17*c*, one dash representing a filament and two bridges extending from it. Notice that the pattern generated in this drawing is very similar to the actual festooned pattern seen in the stereocilia.

There are three tests that would substantiate our interpretation. First, if we cut a section that is thick enough to include at least one repeat of the cross-bridges in a single section, the festooned pattern should disappear and each filament in cross section should appear to have a greater diameter. Second, if we compare the same filament in serial thin sections, the density attributed to the bridges should rotate around the filament in adjacent serial sections. To put it another way, in successive sections the pattern of festooning should appear to shift laterally. This can be appreciated by a close examination

of Fig. 17*a*. In the stippled section, the filament on the extreme left has its bridges extending at 3 and 9 o'clock. In the next section up (assuming an equal section thickness), the bridges from this same filament should extend at 1 and 7 o'clock, and in the third section at 11 and 5 o'clock. Third, if we compare the period of the festooning of one section with that of another sectioned from the same stereocilium at a steeper angle relative to the knife, we should find one repeat in the pattern of bridges. If we increase the angle of the knife relative to the filaments, the pattern of the festooning should repeat in a shorter distance. We have carried out all three tests, (*a*) If the section thickness exceeds 275 Å, the festooning disappears. (*b*) In successive serial sections the pattern of festooning shifts laterally by an amount proportional to the thickness of the section. (*c*) A change in the tilt of the block relative to the knife produces a change in the period of the festooning. These results substantiate our hypothesis that the festooned pattern in thin sections is the result of the cross-bridges between filaments.

CONSEQUENCES OF THIS TYPE OF PACKING: Bundles of actin filaments have been described in a number of systems, e.g., the acrosomal processes of *Limulus* and *Mytilus* sperm (28 and 29, respectively), microvilli of sea urchin eggs (3), filopodia from amoebocytes (6), and needles repolymerized from extracts of sea urchin eggs (14). The filaments in these bundles vary in their degree of order, but seem to have two common features: (*a*) the actin filaments are aligned in register (the crossover points of the actin helices are aligned side by side) and (*b*) they are arranged on a hexagonal lattice (4, 27–29). One of the features of this arrangement is that it maximizes the number of specific cross-links that can be made between filaments in a bundle. The actin, moreover, is found in association with one or more additional proteins that serve to cross-link the filaments together. One of the morphological consequences of using a macromolecular cross-bridge is to increase the distance between filaments as compared with that of a crystal of purified actin filaments held together by ions such as magnesium. For example, in negatively stained images of the acrosomal process of *Limulus* sperm, the apparent spacing is 75 Å (4) and in sea urchin egg extracts it is 75 Å (4), whereas in pure actin paracrystals it is only 57 Å (17). A second consequence of the cross-bridges should be the appearance of periodic striations perpendicular to the long axis of the filament bundle. In all but the acrosomal process of *Limulus* sperm periodic transverse bands spaced at 110- and 130-Å intervals were observed. These bands result from the cross-bridging proteins that bind adjacent filaments only where cross-bridging can be completed. Cross-bridging can occur only every fourth or fifth monomeric unit because of steric difficulties arising from trying to bridge helices together into a hexagonally packed bundle. In the acrosomal process of *Limulus* sperm, the one exception, the cross-bridging protein is bound to every actin unit (4, 29), even though the actual cross-linking occurs at the same intervals as in the other bundles.

In the stereocilia of the ear we have demonstrated that the actin filaments lie slightly out of register in contrast to the bundles mentioned here. In end-on views of thick sections where the festooned pattern is not so distracting (Fig. 7*b*), the actin filaments are not hexagonally arranged; instead, they do not appear to be very regularly ordered, which is confirmed by diffraction patterns of end-on views. The center-to-center spacing of adjacent filaments in transverse sections is 100 Å. This means that there must be an additional cross-bridging protein(s). In longitudinal sections, transverse bands are not seen

and no meridional spot is found in the diffraction patterns, even though such a spot is present in the stereocilia of bird cochlea in which the filaments are also hexagonally packed (Tilney and DeRosier, unpublished observations). From the data presented, however, it is clear that the festooned arrangement is brought about by the cross-bridges, so the question arises as to how they are arranged in longitudinal section so that no meridional spot is seen. One possibility is that in lizard ears every actin unit has an auxiliary protein(s) bound to it as in *Limulus* sperm; it is premature, however, to conclude this without chemical studies.

The puzzle in the lizard stereocilia, and presumably also in mammals, is how the actin filaments are packed. That using six different experimental procedures and/or fixation techniques made no difference to the packing of filaments seen in longitudinal or transverse sections makes it unlikely that we are altering the order by our fixation methods. If, in fact, fixation were not optimal, one would expect to see a lack or reduction of order or a change in the packing with different fixation procedures. By similar arguments it is unlikely that we are "creating" order by fixation because not only is the same degree of order visualized by different fixation techniques, but also it is extremely unlikely that one could form paracrystals that are festooned so rapidly during fixation, because the filaments would have to slide past one another over long distances to get the crossover points of the helices in register and the bridges hooked up.

At this point we are faced with a paradox. The periodic nature of the festooning means that structural features in any one area of the stereocilium are in some sense spatially correlated with those in all other areas, yet there is no regular lattice that would hold these morphological features in register. Instead, in transverse sections the local packing of filaments shows no crystalline regularity even though in longitudinal sections cut from the same blocks the packing appears paracrystalline. The question arises of how cross-bridges can occur regularly between filaments in a structure in which the arrangement of filaments seems to have limited, if any, regularity. It becomes important, then, to determine how a cell can build a rigid, partially ordered structure made of actin filaments and to discover its bonding rules. The primary effect of cross-linking is to increase rigidity, which is indeed a striking property of the acrosomal process of *Limulus* sperm as well as of the stereocilia in the ear. Flock et al. (10) demonstrated, using micromanipulation methods, that the stereocilia of both intact and Triton-extracted hair cells of the vestibular apparatus were rigid and, if bent sharply, would break. They suggested that the "stiffness of the stereocilia depends on the fibrillar core." Our study, by showing that the actin filaments are packed in paracrystalline order that is not changed by a variety of media, extends their report and explains why the bundle is stiff and tends to break rather than bend sharply. From several lines of evidence we conclude that the paracrystalline order in the packing of the filaments must be accounted for by cross-bridges between adjacent filaments. Thus a highly ordered and probably maximally cross-bridged filament bundle would give the stereocilium considerable rigidity; yet because of the dramatic taper, bending should occur at the base of each stereocilium. Thus each stereocilium is designed to behave as a stiff lever that can bend at its base, a conclusion that has been tested experimentally by micromanipulation (10).

One wonders if it is possible to alter the rigidity of the filament bundle. There are two simple possibilities. One would

be to alter the rigidity by a dramatic reduction in the number of cross-bridges and the other by changing the pitch (twist) of the actin filaments in the bundle. The latter is known to occur during the extension of the acrosomal process of *Limulus* sperm (4, 5). Other possibilities, such as the active sliding of filaments past one another, as occurs in cilia, flagella, or muscle, are extremely unlikely because of the cross-linking.

We would like to extend our thanks to Mrs. Pat Connelly who cut some of the initial sections used in this study. Our special thanks go to Emma Jean Battles who processed the tissue and painstakingly cut most of the sections for this report. Her patience is remarkable and without it we could not have proceeded. We would also like to thank Charles Peto and Joseph DiFranza for technical assistance in scanning electron microscopy. Our appreciation goes to Dr. James Saunders who spent time with us in discussions and criticism of this manuscript. We wish to thank Edward Salmon for the design and construction of the optical diffractometer and Dr. Caroline Pond for her help in maintaining the lizards. We particularly wish to thank Dr. Thomas Pollard who, as editor, recommended changes in the manuscript that improved it enormously. We are extremely grateful to him.

This work was supported by the National Science Foundation (grant GB22863 to L. G. Tilney) and the National Institutes of Health (grants GM2189 to D. J. DeRosier and NS12801 to M. J. Mulroy).

Received for publication 18 June 1979, and in revised form 21 March 1980.

REFERENCES

- Bagger-Sjöback, D., and J. Wersäll. 1973. The sensory hairs and tectorial membrane of the basilar papilla in the lizard, *Calotes versicolor*. *J. Neurocytol.* 2:329-350.
- Begg, D. A., R. Rodewald, and L. I. Rebhun. 1978. The visualization of actin filament polarity in thin sections: Evidence for the uniform polarity of membrane-associated filaments. *J. Cell Biol.* 79:846-852.
- Burgess, D. R., and T. E. Schroeder. 1977. Polarized bundles of actin filaments within microvilli of fertilized sea urchin eggs. *J. Cell Biol.* 74:1032-1037.
- DeRosier, D. J., E. Mandelkow, A. Silliman, L. Tilney, and R. Kane. 1977. The structure of actin-containing filaments from two types of non-muscle cells. *J. Mol. Biol.* 113:679-695.
- DeRosier, D. J., L. Tilney, and P. Flicker. 1980. A change in the twist of the actin-containing filaments occurs during the extension of the acrosomal process in *Limulus* sperm. *J. Mol. Biol.* 137:375-389.
- Edds, K. T. 1977. Dynamic aspects of filopodial formation by reorganization of microfilaments. *J. Cell Biol.* 73:479-491.
- Engström, H., and B. Engström. 1978. The structure of the hairs on the cochlear sensory cells. *Hearing Research.* 1:49-66.
- Flock, A. 1971. Sensory transduction in hair cells. In *Handbook of Sensory Physiology*. Vol. 1. Principles of Receptor Physiology. W. R. Lowenstein, editor. Springer-Verlag, Berlin. 396-441.
- Flock, A., and H. C. Cheung. 1977. Actin filaments in sensory hairs of inner ear receptor cells. *J. Cell Biol.* 75:339-343.
- Flock, A., B. Flock, and E. Murray. 1977. Studies on the sensory hairs of receptor cells in the inner ear. *Acta Oto-laryngol.* 83:85-91.
- Hasty, D. L., and E. D. Hay. 1978. Freeze-fracture studies of the developing cell surface. II. Particle-free membrane blisters on glutaraldehyde-fixed corneal fibroblasts are artefacts. *J. Cell Biol.* 78:756-768.
- Hudspeth, J., and D. P. Corey. 1977. Sensitivity, polarity and conductance change in the response of vertebrate hair cells to controlled mechanical stimuli. *Proc. Natl. Acad. Sci. U. S. A.* 74:2407-2411.
- Hull, B. E., and L. A. Staehelin. 1979. The terminal web: A reevaluation of its structure and function. *J. Cell Biol.* 81:67-82.
- Kane, R. I. 1975. Preparation and purification of polymerized actin from sea urchin egg extracts. *J. Cell Biol.* 66:305-315.
- Lowey, S., H. S. Slayter, A. G. Weeds, and A. Baker. 1969. Substructure of myosin by enzyme degradation. *J. Mol. Biol.* 42:1-29.
- Miller, M. R. 1966. The cochlear duct of lizards. *Proc. Calif. Acad. Sci.* 33:255-359.
- Moore, P. B., H. E. Huxley, and D. J. DeRosier. 1970. Three dimensional reconstruction of F-actin, thin filaments, and decorated thin filaments. *J. Mol. Biol.* 50:279-292.
- Mooseker, M. S. 1976. Brush border motility: Microvillar contraction in Triton-treated brush borders isolated from intestinal epithelium. *J. Cell Biol.* 71:417-433.
- Mooseker, M. S., T. D. Pollard, and K. Fujiwara. 1978. Characterization and localization of myosin in the brush border of intestinal epithelial cells. *J. Cell Biol.* 79:444-453.
- Mooseker, M. S., and L. G. Tilney. 1975. Organization of an actin filament-membrane complex. Filament polarity and membrane attachment in the microvilli of intestinal epithelial cells. *J. Cell Biol.* 67:725-743.
- Mulroy, M. J. 1974. Cochlear anatomy of the alligator lizard. *Brain Behav. Evol.* 10:69-87.
- Mulroy, M. J., D. W. Altmann, T. F. Weiss, and W. T. Peake. 1974. Intracellular electric responses to sound in a vertebrate cochlea. *Nature (Lond.)* 249:482-485.
- Murray, J. M. 1973. Cooperative alterations in the behavior of contractile proteins. PhD thesis, University of Pennsylvania.
- Nadol, J. B., M. J. Mulroy, D. A. Goodenough, and T. F. Weiss. 1976. Tight and gap junctions in a vertebrate inner ear. *Am. J. Anat.* 147:281-301.

25. Reedy, M. K. 1968. Ultrastructure of insect flight muscle. I. Screw sense and structural groupings in the rigor cross-bridge lattice. *J. Mol. Biol.* 31:155-176.
26. Rodewald, R., S. B. Newman, and M. J. Karnovsky. 1976. Contractions of isolated brush borders from intestinal epithelium. *J. Cell Biol.* 70:541-554.
27. Spudich, J. A., and L. A. Amos. 1979. Structure of actin bundles from microvilli of sea urchin eggs. *J. Mol. Biol.* 129:319-331.
28. Tilney, L. G. 1975. The role of actin in non-muscle cell motility. In *Molecules and Cell Movement*. S. Inoué and R. Stephens, editors. Raven Press, New York. 339-388.
29. Tilney, L. G. 1975. Actin filaments in the acrosomal reaction of *Limulus* sperm: Motion generated by alterations in the packing of the filaments. *J. Cell Biol.* 64:289-301.
30. Tilney, L. G., and R. Cardell, Jr. 1970. Factors controlling the reassembly of the microvillus border of the small intestine of the salamander. *J. Cell Biol.* 47:408-422.
31. Weiss, T. F., M. J. Mulroy, R. G. Turner, and C. L. Pike. 1976. Auditory responses of single cochlear nerve fibers of the alligator lizard. *Brain Res.* 115:71-90.